Analog Integrated Circuits and Signal Processing (2021) 108:69–74
https://doi.org/10.1007/s10470-021-01861-8

Ultra-wide stopband microstrip lowpass filter using lumped element equivalent circuit

Abbas Alipour[1] · Akram Sheikhi[1]

Received: 30 November 2020 / Revised: 30 November 2020 / Accepted: 24 April 2021 / Published online: 7 May 2021

Abstract
In this paper, a microstrip filter using a modified stepped impedance resonator with high return loss, low insertion loss, and ultra-wide stopband is presented. The frequency response of the filter based on the layout and LC model is presented. The presented LPF consists of stepped impedance resonators to achieve a − 20 dB suppression level from 3.26 GHz up to 30 GHz. Using stepped impedance resonators results in multiple transmission zeros in the stopband. The proposed filter has an insertion loss of 0.1 dB, return loss of 26 dB, and cut-off frequency of 3 GHz. The transition band of the filter (with attenuation levels of − 3 dB and − 20 dB) is 0.26 GHz. The simulated results are close to the measured results, which shows the accuracy of our design.

Keywords Microstrip filter · Stepped impedance resonator · And ultra-wide stopband

1 Introduction

The Wireless communication systems are used lowpass filters (LPFs) to eliminate unwanted frequencies and suppression harmonics. The LPFs with good features such as wide stopband and low losses are necessary to reach a high data rate communication system with a low system error rate (SER) [1]. Recently, different methods have been proposed to improve the performance of LPFs [2–15]. Defected ground structure (DGS) in the combination of spiral defected microstrip structure (DMS) has been used to design the LPF with poor performances of low return loss and narrow stop bandwidth [2]. In [3], the filter using defected structure has high harmonic suppression and low selectivity. The filter described in [4], has high rejection in the stopband region. However, along with high rejection, other characteristics such as high return loss are also essential for communication systems. The DGS with an inherent bandgap has been used to achieve wide stopband characteristics and compact size [5]. However, these structures are suffered from the complexity of fabrication compared to conventional LPFs. In [6], LPFs with microstrip coupled-line hairpin resonator and interdigital capacitor with gradual cut-off frequency and narrow stop bandwidth has been proposed. We can consider the several disadvantages of high insertion loss (IL) and low return loss (RL) for the proposed filter in [7]. However, the LPF in [8] has a wide stop bandwidth, but the performance of the filter has been restricted by RL and IL. Stepped impedance resonators (SIRs) and hexangular patches have been utilized to reach a high suppression level in the stopband region [9, 10]. The elimination of harmonics in high frequency circuits could be obtained by suppressing cell. The miniaturized suppressing cell has been integrated with the lowpass filter to suppress the harmonics [11]. Gradual cut-off frequency and ultra-wide stopband are characteristics of the proposed LPF in [12]. In [13], a theoretical analysis of a microstrip lowpass filter using split resonators is developed. To expand the stopband region and harmonic suppression, multiple open stubs have been used. A LPF presented in [14], has a high roll-off rate and wide stopband. However, this LPF has low return loss and low stopband rejection. A wide stopband LPF using Triangle Shaped Resonators with flat group delay as its advantage and low return loss as its disadvantage has been presented in [15]. In [16], a miniaturized LPF using cylindrical-shaped resonators for integrated applications is

✉ Akram Sheikhi
Sheikhi.a@lu.ac.ir

[1] Department of Electronics, Faculty of Engineering, Lorestan University, Khorram-Abad, Iran

introduced, but it suffers from high return loss and complex configuration. Triangular and rectangular shaped resonator are used to achieve ultra-wide stopband and sharp roll-off microstrip low pass [17]. In this paper, a wide stopband lowpass filter using modified stepped impedance resonator with high selectivity, RL better than 26 dB, and IL lower than 0.1 dB is proposed. Also, the LC equivalent circuit of each structure is presented. The different SIRs are used to achieve a -20 dB attenuation level in the stopband region from 3.26 to 30 GHz.

2 The modified stepped impedance resonator

The schematic and equivalent circuit of the proposed resonator is shown in Fig. 1a, b, respectively. The dimension of the resonator is $g_0 = 0.1$, $w_0 = 0.1$, $w_1 = 0.2$, $w_2 = 5.4$, $w_3 = 5.85$, $l_1 = 6.87$ and $l_2 = 0.6$, $l_3 = 5$ and $l_4 = 0.3$ (all dimensions are in mm). L_i (i = 1, 2, 3, 4, 5) and C_i (i = 1, 2, 3, 4, 5) are the equivalent lumped element circuit. The equivalent inductors and capacitors have been obtained from [1] as:

$$L_i = \frac{1}{\omega} Z_{si} \sin\left(\frac{2\pi}{\lambda_g} l_i\right) \tag{1}$$

and

$$C_i = \frac{1}{\omega} \frac{1}{Z_{si}} \tan\left(\frac{\pi}{\lambda_g} l_i\right) \tag{2}$$

and the open stub equivalent capacitance is

$$C_{oi} = \frac{\sqrt{\varepsilon_{eff}}}{C Z_{si}} l_i \tag{3}$$

where Zsi, li, and λg are the characteristic impedance, length, and the guided wavelength, respectively. By using the presented equations, we can compute the value of these parameters. The calculated values are shown in Table 1. Figure 1c shows the S21 parameter of the LC equivalent circuit and the proposed resonator. A good agreement between the frequency response of the LC model and EM simulation is obtained. To investigate the resonator's performance, the frequency response in the different amounts of l3 is shown in Fig. 1d. Obviously, by increasing the value of l3 the transmission zero (TZ) at 8.16 GHz is shifted to the right-hand side. So, the dimension of the rectangular patch (l3 and w2) in Fig. 1a (its equivalent circuit is (L_3-L_4-C_4) in Fig. 1b) has a main effect on the

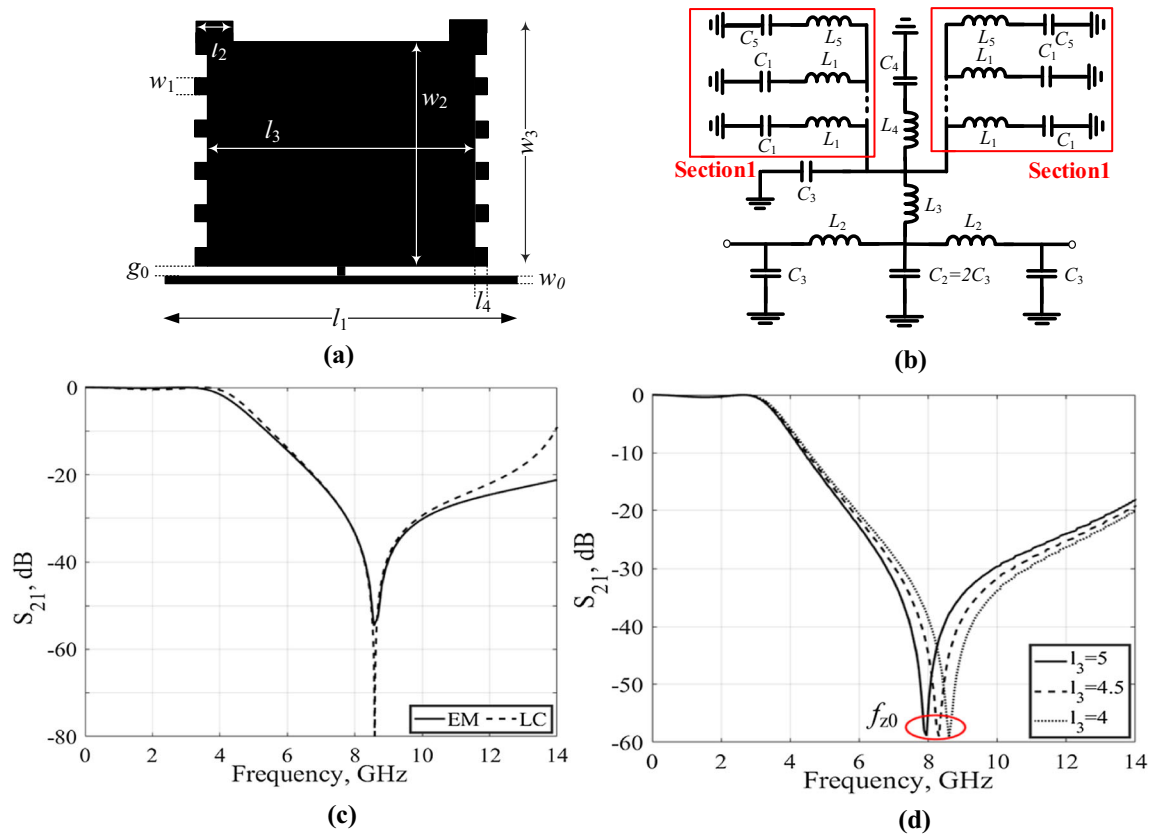

Fig. 1 **a** Layout **b** LC equivalent circuit, **c** simulation results, and **d** S21 as a function of l3

Table 1 Values of the LC circuit

Parameters	L_1 (nH)	L_2 (nH)	L_3 (nH)	L_4 (nH)	L_5(nH)	C_1 (fF)	C_3 (pF)	C_4 (pF)	C_5 (fF)
Calculated	0.18	3.42	0.16	0.5	0.15	3.1	0.04	0.45	6.58
Optimized	0.22	3.15	0.121	0.67	0.13	4.35	0.1	0.3	7.36

location of fz0. Also, Fig. 1b shows that the frequency of transmission zeroes have been controlled by (L_3-L_4-C_4), (L_3-L_1-C_1), (L_3-L_5-C_5).

Two folded stepped impedance resonators (SIR) have been added to the resonator to improve the transition band, Fig. 2a. The physical dimensions of the proposed structure are: w4 = 4.5, l5 = 1.5, g1 = 0.8, g2 = 0.15, θ = 30° and g3 = 0.2 (all dimensions in mm). In Fig. 2b, Sect. 2, which consists of L6, L7, L8, C6, C7 and C8, is the LC equivalent circuit of the folded SIRs. More transmission zeros in stopband can be achieved by the folded SIRs. As can be seen, the extra transmission zeros can be obtained by LC resonant-circuits (L6, L7, L8, C6, C7, and C8). The comparison between the LC and EM simulation is shown in Fig. 2c. Also, the variations of fz1 and fz2 of the proposed structure as a function of l5 are shown in Fig. 2d. It is clear that the fz1 decreases by increasing l5, and fz2 increases by increasing l5. The values of the LC model are given in Table 2.

The addition of modified SIR results in a better attenuation level in the stopband region, Fig. 3a. The frequency response shows two transmission zero at fz1 = 3.65 GHz and fz2 = 6.2 GHz. With the addition of a SIR between folded SIRs, second transmission zero at 8.2 GHz is shifted to 6.2 GHz. The lumped equivalent circuit, and the simulation results are shown in Fig. 3b, c, respectively.

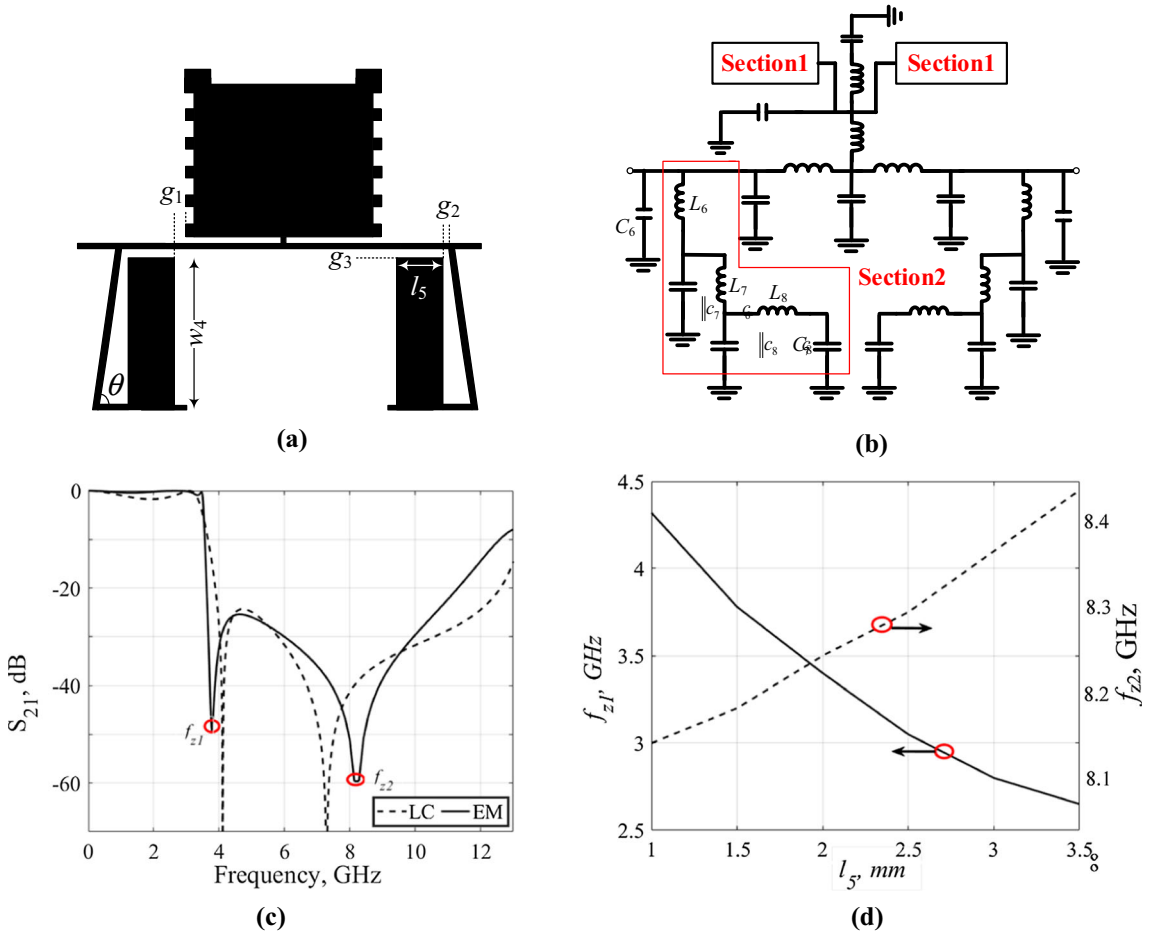

Fig. 2 **a** Layout, **b** LC equivalent circuit, **c** simulation results, **d** fz1 and fz2 versus l5

Table 2 Calculated and optimized values of the LC equivalent circuit

Parameters	L_6(nH)	L_7(nH)	L_8(nH)	C_6(pF)	C_7(fF)	C_8(fF)
Calculated	3.42	0.72	1.0	0.63	12	0.19
Optimized	2.7	0.97	1.2	1.04	10	0.15

3 Simulation and measurement results

The addition of two folded SIRs at the upper side of the structure in Fig. 3a results in the final LPF. Figure 4a, b shows the final schematic and photograph of the filter. The dimensions of 50-Ω matching lines are wf = 1.56 mm and lf = 1 mm for the substrate with εr = 2.2 and h = 0.7874 mm. In Fig. 4c, the simulated and measured results of the LPF have been shown. It is obvious that all harmonics are controlled, and the attenuation level is good. As shown in Fig. 4d, the group delay of the proposed filter is less than 0.65 ns. For matching at the input and output ports, two microstrip lines are used as a 50-Ω matching network. The final schematic of the proposed LPF has been simulated by ADS 2014, and scattering parameters are measured by HP 8510B network analyzer. Finally, the stopband region up to 30 GHz with − 20 dB suppression level has been obtained. Also, the exclusive size is only 14.38 mm × 12 mm that is equal to 0.161λg × 0.133λg. On the other hand, the designed filter with compact size can reduce the voltage standing wave ratio (VSWR) and IL. Table 3 compares the performance of the filter as IL, RL, relative stop bandwidth (RSB), suppression factor (SF), band rejection, and circuit size in comparison to other works. Table 3 shows that the proposed LPF has a compact size, low insertion loss, high return loss, and ultra-wide stopband.

4 Conclusion

In this paper, a novel wide stopband LPF by SIRs with fc = 3 GHz was designed, fabricated, and measured. Our approach framework realizes Sharp transition band, low IL, high RL and wide stopband. We proposed LC equivalent circuits for the SIRs. Finally, a wide stopband LPF based on SIRs is realized. The − 20 dB stopband rejection, IL of

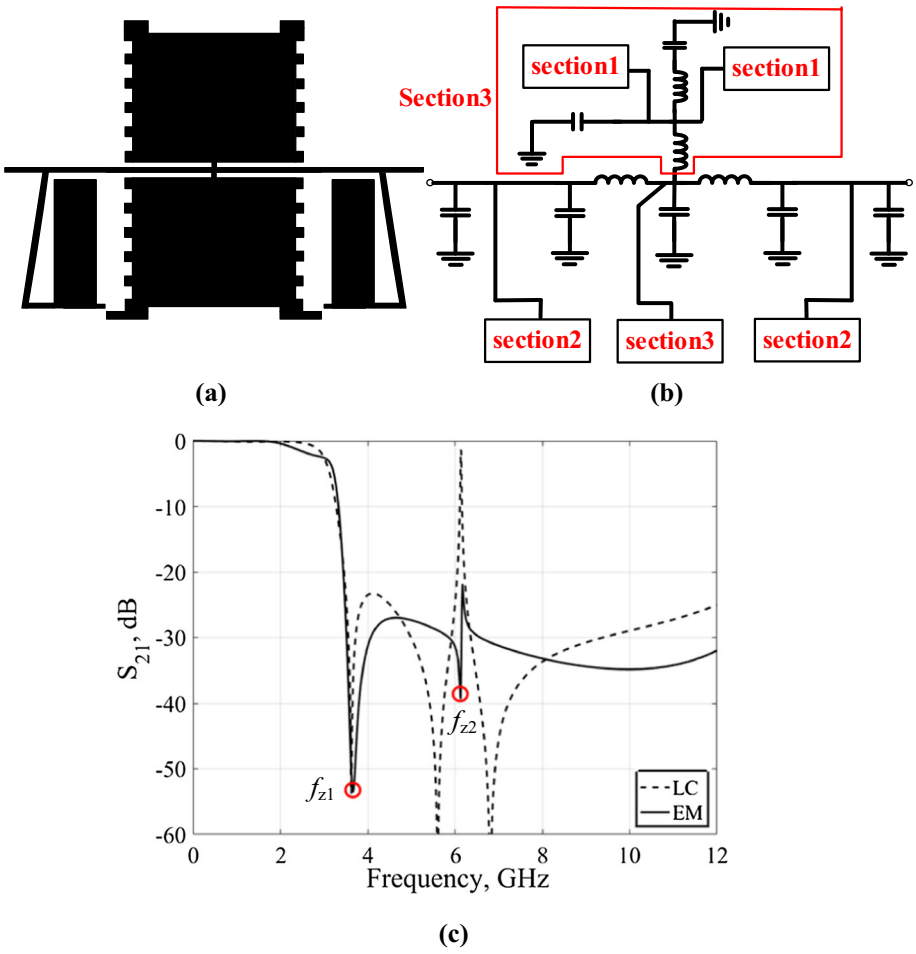

Fig. 3 **a** Layout, **b** LC equivalent circuit, and **c** simulation results

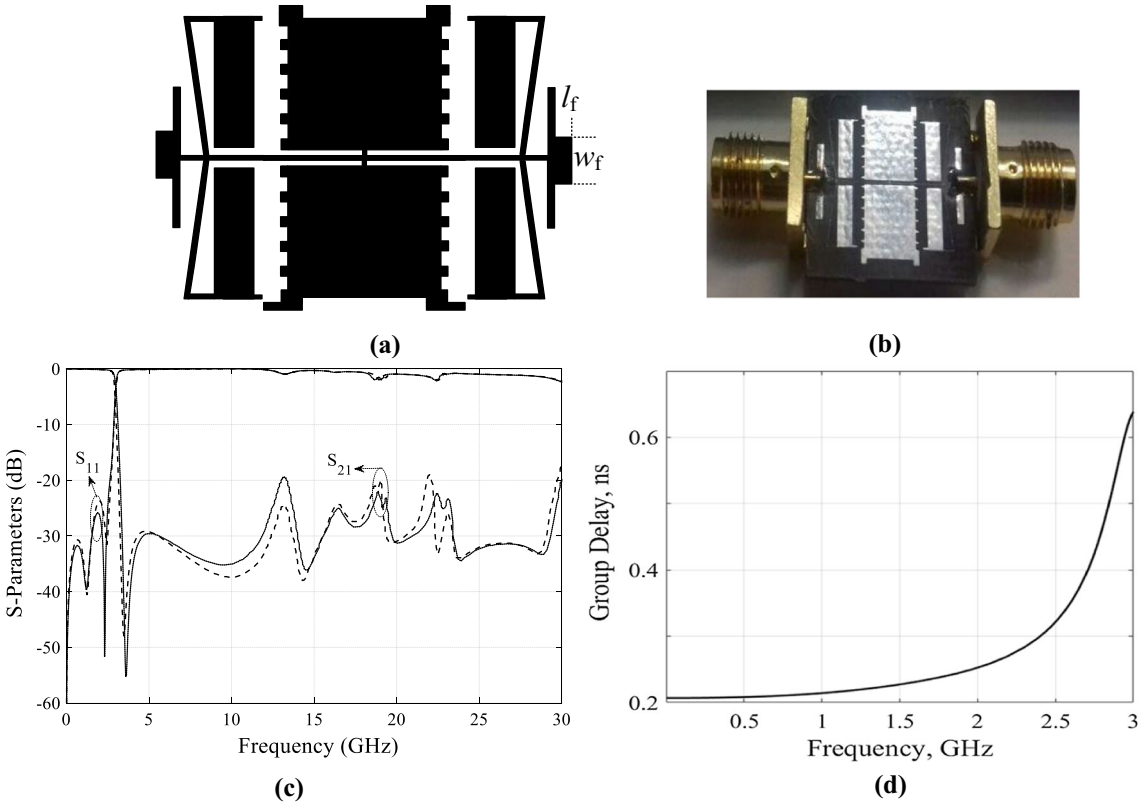

Fig. 4 **a** Final schematic, **b** photograph, **c** simulated (solid) and measured (dash) results, **d** Simulated group delay

Table 3 the comparison with other works

Reference no.	f_c (GHz)	RSB (%)	IL (dB)	RL (dB)	Band rejection	Circuit size* (λ_g^2)
[3]	2.4	85.7	0.35	11	− 20 dB up to 6 GHz	0.07
[4]	1.5	112.5	0.7	17	− 20 dB up to 7.5 GHz	0.161
[5]	2.11	159	–	10	− 15 dB up to 20 GHz	0.021
[6]-I	2.5	69	0.45	14	− 20 dB up to 11.8 GHz	0.149
[6]-II	2.5	114	0.45	14	− 20 dB up to 11.8 GHz	0.179
[7]	2.4	135.5	0.6	12	− 20 dB up to 15 GHz	0.038
[8]	3.12	135	0.33	11.54	− 20 dB up to 19 GHz	0.062
[9]	2.68	150	0.18	18	− 20 dB up to 22 GHz	0.019
'[11]	3.8	134	0.1	14	− 20 dB up to 20 GHz	0.018
[12]	0.9	157	0.5	15.5	− 20 dB up to 16 GHz	0.018
[13]	2.9	156	0.1	17.5	− 20 dB up to 25 GHz	0.042
[14]	1.95	155	0.4	12	− 15 dB up to 16 GHz	0.033
[16]	4.39	-	0.1	18	− 20 dB up to 30 GHz	–
This Work	3.0	161	0.1	26	− 20 dB up to 30 GHz	0.021

0.1 dB, and RL higher than 26 dB has been obtained. As to the stopband region, the stop bandwidth from 3.26 GHz up to 30 GHz is achieved. The LPF, with these good characteristics, will open up novel avenues for use in modern wireless communication systems.

References

1. Hong, J. S., & Lancaster, M. J. (2001). *Microstrip filters for RF/microwave applications*. New York: Wiley.
2. Mondal, P., Dey, H., & Parui, S. K. (2015). Design of microstrip lowpass filter in combination with defected ground and defected microstrip structures. *Computational Advancement in Communication Circuits and Systems, 33*(5), 61–66.
3. Sarbani, S., Tamasi, M., & Dwipjoy, S. (2018). Modelling and validation of microwave LPF using modified rectangular split ring resonators (SRR) and defected structures. *International Journal of Electronics and Communications (AEU), 88*, 1–10.
4. Hammed, R., Hassan, S.,& Ajeel, S. (2020). Compact microstrip lowpass filter with high harmonics suppression using defected structures. *International Journal of Electronics and Communications (AEU)*, *115*(5), 1530–1532.
5. Tu, W.-H., & Chang, K. (2005). Compact microstrip lowpass filter with sharp rejection. *IEEE Microwave and Wireless Component Letters, 15*(5), 404–406.
6. Luo, S., Zhu, L., & Sun, S. (2008). Stopband-expanded lowpass filters using microstrip coupled-line hairpin units. *IEEE Microwave and Wireless Component Letters, 18*(8), 506–508.
7. Li, J.-L., Qu, S.-W., & Xue, Q. (2009). Compact microstrip lowpass filter with sharp roll-off and wide stop-band. *Electronic Letters, 45*(2), 110–111.
8. Hayati, M., Sheikhi, A., & Lotfi, A. (2010). Compact lowpass filter with wide stopband using modified semi-elliptic and semi-circular microstrip patch resonator. *Electronic Letters, 46*(22), 1507–1509.
9. Sheikhi, A., Alipour, A., & Abdipour, A. (2017). Design of compact wide stopband microstrip lowpass filter using T-shaped resonator. *IEEE Microwave and Wireless Component Letters, 27*(2), 111–113.
10. Sheikhi, A., Alipour, A., & Hemesi, H. (2017). Design of microstrip wide stopband lowpass filter with lumped equivalent circuit. *Electronic Letters, 53*(21), 1116–1118.
11. Heidari, B., & Shama, F. (2018). A harmonics suppressed microstrip cell for integrated applications. *AEU International Journal of Electronics and Communications (AEU)*, *83*, 519–522.
12. Chen, F. C., Li, R. S., & Chu, Q. X. (2017). Ultra-wide stopband lowpass filter using multiple transmission zeros. *IEEE Access: Practical Innovations, Open Solutions, 5*, 6437–6443.
13. Nisamol, T. A., Abdulla, P., & Raphika, P. M. (2020). Dual split resonator lowpass filter with ultra-wide stopband and sharp roll-off rate. *IET Microwaves, Antennas & Propagation*, *14*(12), 1462–1468.
14. Kumar, L., & Parihar, M. S. (2018). A wide stopband lowpass filter with high roll-off using stepped impedance resonators. *IEEE Microwave and Wireless Components Letters, 28*(5), 404–406.
15. Kolahi, A., & Shama, F. (2018). Compact microstrip low pass filter with flat group-delay using triangle-shaped resonators. *AEU-International Journal of Electronics and Communications (AEU)*, *83*, 433
16. Tahmasbi, M., Razaghian, F., & Roshani, S. (2019). Design of compact microstrip low pass filter using triangular and rectangular shaped resonator with ultra-wide stopband and sharp roll-off. *Analog Integrated Circuits and Signal Processing, 101*(1), 99–107.
17. Amin, I. M. et al. (2018). Miniaturized microstrip lowpass filter using cylindrical-shaped resonators for integrated applications. *Analog Integrated Circuits and Signal Processing, 95*(2), 223–229.

Abbas Alipour was born in Ahvaz, Khuzestan in 1991. He received his B.Sc. degree in Electronic Engineering from Islamic Azad University, Shushtar Branch, Khuzestan, Iran, in 2012, and his M.S. degree from Lorestan University, Iran, in 2016. He is currently an electronic Ph.D. student at Lorestan University. He jointed to instrument engineering group of MIS petrochemical company in 2019. The fields of his interest are optical communication systems, design of optical networks, design of microwave device include lowpass and bandpass filter and Plasmonics, Metamaterials, Optical Sensors. He has authored and co-authored 14 peer-reviewed journals and 12 conference papers.

Akram Sheikhi was born in Khorramabad, Iran in 1985. She received the B.E. degree from Shariaty University, Tehran, Iran, in 2007 and the M.Sc. and Ph.D. degrees in Electrical Engineering from Razi University, Kermanshah, Iran, in 2010 and 2014, respectively. She is currently an Associate Professor with the Department of Electrical Engineering, Lorestan University, Khorramabad, Iran. Her research interests include microwave circuits, high-efficiency power amplifiers, and wireless power transfer systems.